Influence of Ring Annelation on the Mode Selectivity of the Ionized Diazabicycloheptenes and Corresponding Housanes: An ESR and ENDOR Study

by **Fabian Gerson*** and **Coşkun Şahin***[1])

Institut für Physikalische Chemie der Universität Basel, Klingelbergstrasse 80, CH-4056 Basel

Dedicated to Professor *Edgar Heilbronner* on the occasion of his 80th birthday

The tricyclic azoalkanes, (1α,4α,4aα,7aα)-4,4a,5,6,7,7a-hexahydro-1,4,8,8-tetramethyl-1,4-methano-1*H*-cyclopenta[*d*]pyridazine (**1c**), (1α,4α,4aα,6aα)-4,4a,5,6,6a-pentahydro-1,4,7,7-tetramethyl-1,4-methano-1*H*-cyclobuta[*d*]pyridazine (**1d**), (1α,4α,4aα,6aα)-4,4a,6a-trihydro-1,4,7,7-tetramethyl-1,4-methano-1*H*-cyclobuta[*d*]pyridazine (**1e**), and (1α,4α,4aα,5aα)-4,4a,5,5a-tetrahydro-1,4,6,6-tetramethyl-1,4-methano-1*H*-cyclopropa[*d*]pyridazine (**1f**), as well as the corresponding housanes, the 2,3,3,4-tetramethyl-substituted tricyclo[3.3.0.0^{2,4}]octane (**2c**), tricyclo[3.2.0.0^{2,4}]heptane (**2d**), and tricyclo[3.2.0.0^{2,4}]hept-6-ene (**2e**), were subjected to γ-irradiation in *Freon* matrices. The reaction products were identified with the use of ESR and, in part, ENDOR spectroscopy. As expected, the strain on the C-framework increases on going from the cyclopentane-annelated azoalkanes and housanes (**1c** and **2c**) to those annelated by cyclobutane (**1d** and **2d**), by cyclobutene (**1e** and **2e**), and by cyclopropane (**1f**). Accordingly, the products obtained from **1c** and **2c** in all three *Freons* used, $CFCl_3$, CF_3CCl_3, and $CF_2ClCFCl_2$, were the radical cations **3c**$^{\cdot+}$ and **2c**$^{\cdot+}$ of 2,3,4,4-tetramethylbicyclo[3.3.0]oct-2-ene and 2,3,3,4-tetramethylbicyclo[3.3.0]octane-2,4-diyl, respectively. In $CFCl_3$ and CF_3CCl_3 matrices, **1d** and **2d** yielded analogous products, namely the radical cations **3d**$^{\cdot+}$ and **2d**$^{\cdot+}$ of 2,3,4,4-tetramethylbicyclo[3.2.0]hept-2-ene and 2,3,3,4-tetramethylbicyclo[3.2.0]heptane-2,4-diyl. The radical cations **3c**$^{\cdot+}$ and **3d**$^{\cdot+}$ and **2c**$^{\cdot+}$ and **2d**$^{\cdot+}$ correspond to their non-annelated counterparts **3a**$^{\cdot+}$ and **3b**$^{\cdot+}$, and **2a**$^{\cdot+}$ and **2b**$^{\cdot+}$ generated previously under the same conditions from 2,3-diazabicyclo[2.2.1]hept-2-ene (**1a**) and bicyclo[2.1.0]pentane (**2a**), as well as from their 1,4-dimethyl derivatives (**1b** and **2b**). However, in a $CF_2ClCFCl_2$ matrix, both **1d** and **2d** gave the radical cation **4d**$^{\cdot+}$ of 2,3,3,4-tetramethylcyclohepta-1,4-diene. Starting from **1e** and **2e**, the radical cations **4e**$^{\cdot+}$ and **4e′**$^{\cdot+}$ of the isomeric 1,2,7,7- and 1,6,7,7-tetramethylcyclohepta-1,3,5-trienes appeared as the corresponding products, while **1f** was converted into the radical cation **4f**$^{\cdot+}$ of 1,5,6,6-tetramethylcyclohexa-1,4-diene which readily lost a proton to yield the corresponding cyclohexadienyl radical **4f**$^{\cdot}$. Reaction mechanisms leading to the pertinent radical cations are discussed.

Introduction. – In a previous work, ionization of 2,3-diazabicyclo[2.2.1]hept-2-ene (**1a**) and the corresponding bicyclo[2.1.0]pentane (housane; **2a**), as well as of their 1,4-dimethyl derivatives **1b** and **2b**, respectively, was carried out by γ-irradiation in *Freon* matrices, and the resulting radical cations were studied by ESR spectroscopy [1]. Whereas the azoalkanes **1a** and **1b** yielded the radical cations of cyclopentene (**3a**) and its 1,3-dimethyl derivative **3b**, respectively, cyclopentane-1,3-diyl radical cations were obtained by starting from the corresponding housanes **2a** and **2b** (*Scheme 1*).

Despite a considerable weakening of the central bond between the bridgehead C-atoms in **2a** and **2b**, the geometric integrity of the parent housanes was retained in the cyclopentane-1,3-diyl radical cations, which are, therefore, denoted **2a**$^{\cdot+}$ and **2b**$^{\cdot+}$. In

---

[1]) Present address: *Boehringer Ingelheim Pharma KG*, Birkendorfer Strasse 65, D-88397 Biberach an der Riss.

Scheme 1

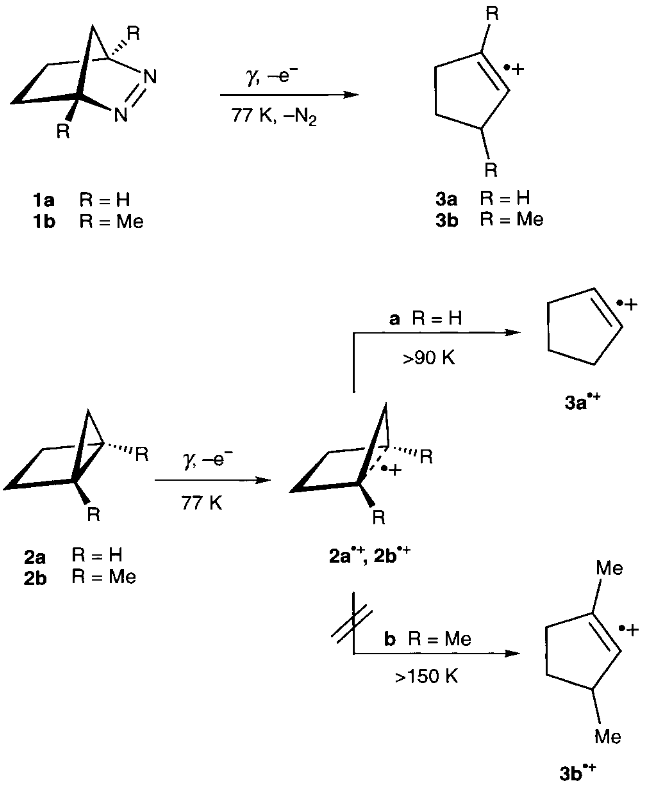

general, such diyl radical cations exhibited a high tendency to rearrange by 1,2-H or alkyl shift to respective cyclopentene radical cations like **3a**$^{\cdot+}$ and **3b**$^{\cdot+}$, as confirmed by photoinduced and chemical electron-transfer studies (PET and CET) in fluid solution [2]. Thus, **2a**$^{\cdot+}$ in CF_3CCl_3 matrix isomerized above 90 K to **3a**$^{\cdot+}$ by a 1,2-H shift from the *syn*-5 position, a result established by stereolabeling of **2a**$^{\cdot+}$ [1c]. In contrast, **2b**$^{\cdot+}$ proved to be exceedingly resistent to an analogous rearrangement to **3b**$^{\cdot+}$, even at 150 K, the softening point of the $CFCl_3$ matrix [1d]. According to ESR studies, an activation energy of, at least, 40 kJ mol^{-1} (*ca.* 10 kcal mol^{-1}) is required for this rearrangement.

In the conversion of the azoalkanes **1a** and **1b** to the radical cations **3a**$^{\cdot+}$ and **3b**$^{\cdot+}$ of cyclopentenes, respectively, the primary radical cations **1a**$^{\cdot+}$ and **1b**$^{\cdot+}$ should extrude N_2 by stepwise cleavage of the two C–N bonds to yield C-centered species. Such a pathway is in line with the well-accepted finding that extrusion of N_2 from bicyclic azoalkanes proceeds by a two-step mechanism with diazenyl diradicals as *bona fide* intermediates [2a][3]. Like these diradicals, the corresponding radical cations may expel N_2 with a concomitant 1,2-H or alkyl shift through a backside attack on the remaining C–N bond. The failure to observe the ESR spectra not only of the labile cyclopentane-1,3-diyl radical cation **2a**$^{\cdot+}$ but also of its relatively persistent 1,3-dimethyl derivative **2b**$^{\cdot+}$, when starting from the corresponding azoalkanes **1a** and **1b**, is noteworthy. It indicates that the reaction path of these azoalkanes to the cyclopentene radical cations **3a**$^{\bullet+}$ and **3b**$^{\bullet+}$ does not proceed exclusively *via* **2a**$^{\bullet+}$ and **2b**$^{\bullet+}$, respectively.

The differing final products of the azoalkanes and the housanes upon their ionization by γ-rays in *Freon* matrices and, in particular, the striking resistance of **2b**$^{\bullet+}$ to rearrangement prompted us to apply this radiolytic treatment to a series of ring-annelated derivatives of **1b** and **2b**, such as **1c**–**1f** and **2c**–**2e**, to assess whether the strain on the C-framework has an impact on their chemical behavior.

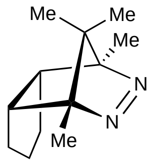

1c

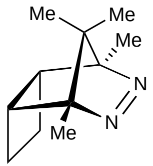

1d

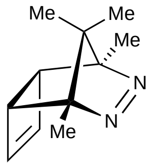

1e

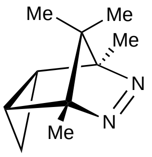

1f

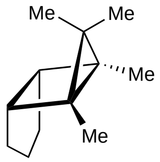

2c

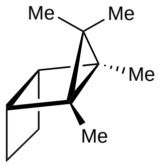

2d

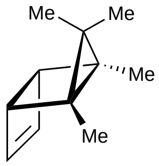

2e

Experimental. – *Synthesis of Starting Materials.* (1α,4α,$4a\alpha$,$7a\alpha$)-4,4a,5,6,7,7a-Hexahydro-1,4,8,8-tetramethyl-1,4-methano-1*H*-cyclopenta[*d*]pyridazine (**1c**), (1α,4α,$4a\alpha$,$6a\alpha$)-4,4a,5,6,6a-pentahydro-1,4,7,7-tetramethyl-1,4-methano-1*H*-cyclobuta[*d*]pyridazine (**1d**), (1α,4α,$4a\alpha$,$6a\alpha$)-4,4a,6a-trihydro-1,4,7,7-tetramethyl-1,4-methano-1*H*-cyclobuta[*d*]pyridazine (**1e**), and (1α,4α,$4a\alpha$,$5a\alpha$)-4,4a,5,5a-tetrahydro-1,4,6,6-tetramethyl-1,4-methano-1*H*-cyclopropa[*d*]pyridazine (**1f**) were prepared according to known procedures [4][5]. The housane derivatives, the 2,3,3,4-tetramethyl-substituted tricyclo[3.3.0.0^{2,4}]octane (**2c**) [5c], tricyclo[3.2.0.0^{2,4}]heptane (**2d**) [4], and tricyclo[3.2.0.0^{2,4}]hept-6-ene (**2e**) [4] were obtained by photolysis ($\lambda > 300$ nm) of the corresponding azoalkanes, **1c**, **1d**, and **1e**, resp., in the ESR tubes containing a soln. of the compound in a *Freon* matrix. 1,5,6,6-Tetramethylcyclohexa-1,4-diene (**4f**) was obtained by photolysis ($\lambda > 300$ nm) of azoalkane **1f** in $CDCl_3$ and was identified by its NMR spectrum. ^{1}H-NMR ($CDCl_3$, 250 MHz): 1.13 (*s*), 1.74 (br. *s*), 2.57 (*m*, H–C(3)), 5.40 (*m*, H–C(2), H–C(4)).

Generation and ESR Studies of Paramagnetic Products. Ionization of **1a**–**1f** and **2a**–**2e** was performed on their ca. 0.01M soln. in $CFCl_3$, CF_3CCl_3, and $CF_2ClCFCl_2$ matrices by γ-irradiation with a ^{60}Co source at 77 K. The total dose amounted usually to 0.5–0.7 Mrad (1 Mrad = 10 kGy; 1 Gy corresponds to 1 J kg^{-1}) and the rate was *ca.* 40 krad/h with exposure times of 12–18 h. The samples in the *Spectrosil*-quartz tube were prepared by the standard-vacuum technique. After γ-irradiation, the sample tube was transferred into the variable-temperature *Dewar* insert within the cavity of a *Bruker-ESP-300* system at an initial temp. of 95 K. ESR spectra were then recorded at 5–10 K intervals over the range of 95 K to the softening points of the matrices. Spectral changes on sample annealing were monitored and checked for reversibility by recycling to the lower temp. In this way, it was possible to differentiate between an irreversible reaction of the radical cation and a reversible change due only to an improvement in the spectral resolution at higher temp. The *g* factors of all paramagnetic species amounted to 2.0030 ± 0.0005.

The radical cations (and the subsequently formed neutral radicals) were, in general, also studied by the ENDOR technique, integrated into the *Bruker-ESP-300* system. Most readily observed signals were those from β-protons²) of freely rotating Me substituents; they had the anisotropic shape characteristic of such protons with

---

²) In ESR spectroscopy, protons separated from a π-center by 0, 1, 2, … sp^3-hybridized C atoms are denoted $\alpha, \beta, \gamma, \ldots$

a positive coupling constant $a = 1/3\ (2A_{\perp} + A_{\parallel})$ where $A_{\perp}$ and $A_{\parallel}$ refer to anisotropic features of an axial hyperfine tensor [6] [7]. The frequency, υ_{H}, of the free proton was 14.5 MHz. Computer simulations of the ESR spectra were fitted to the experimental derivative curve with the aid of the program NIEHS-WinSIM (Public EPR Software Tools, USA, 1996).

Results. – *Cyclopentane Annelation:* **1c** *and* **2c**. *Fig. 1,a*, shows the ESR spectrum observed upon γ-irradiation of the cyclopentane-annelated azoalkane **1c** in a $CFCl_3$ matrix. For the computer simulation (*Fig. 1,b*), the $|a|$ values of ^{1}H-coupling constants were derived from the corresponding ENDOR spectrum (*Fig. 1,c*). The low- and high-frequency components of the ENDOR signals at 6.5–9.5 and 35.5–38.5 MHz, which have an anisotropic shape, arise from β-protons2) in two non-equivalent Me substituents. Amplification of this ENDOR spectrum revealed additional signals at 24–26 and 68–70 MHz representing high-frequency components from two protons. The $|a|$ values of 3.89 (1 H), 1.65 (3 H), 1.52 (3 H), and 0.76 mT (1 H) used in the simulation identify the radical cation as that of 2,3,4,4-tetramethylbicyclo[3.3.0]oct-2-ene (diquinane; **3c**, *Scheme 2*).

Scheme 2

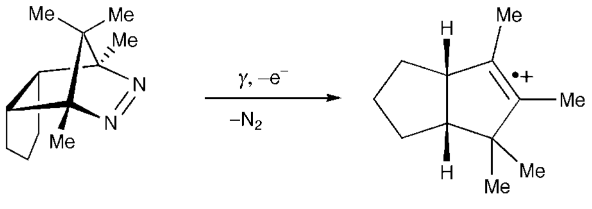

1c **3c**$^{\cdot+}$

Starting from the cyclopentane-annelated housane **2c** in a CF_3CCl_3 matrix, γ-irradiation led to the ESR spectrum displayed in *Fig. 2,a*. Its computer simulation (*Fig. 2,b*) again relied on the $|a|$ values derived from the corresponding ENDOR spectrum (*Fig. 2,c*). The low- and high-frequency components of the ENDOR signals at 7.4–8.5 and 36.4–37.5 MHz have an anisotropic shape similar to that observed for **3c**$^{\cdot+}$ (*Fig. 1,a*); they are due to six β-protons of two equivalent Me substituents. Upon amplification of the ENDOR spectrum, low-frequency components of an additional signal appeared at 21–24 MHz. The simulation was based on the $|a|$ values of 2.91 (2 H), 1.59 (6 H), and 0.55 mT (2 H), which are diagnostic of the radical cation **2c**$^{\cdot+}$ of 2,3,3,4-tetramethylbicyclo[3.3.0]octane-2,4-diyl (*Scheme 3*).

Scheme 3

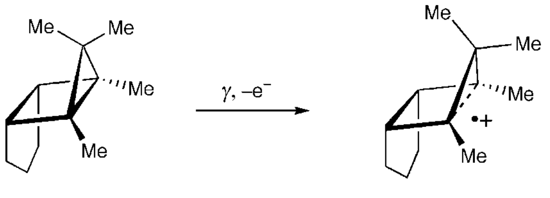

2c **2c**$^{\cdot+}$

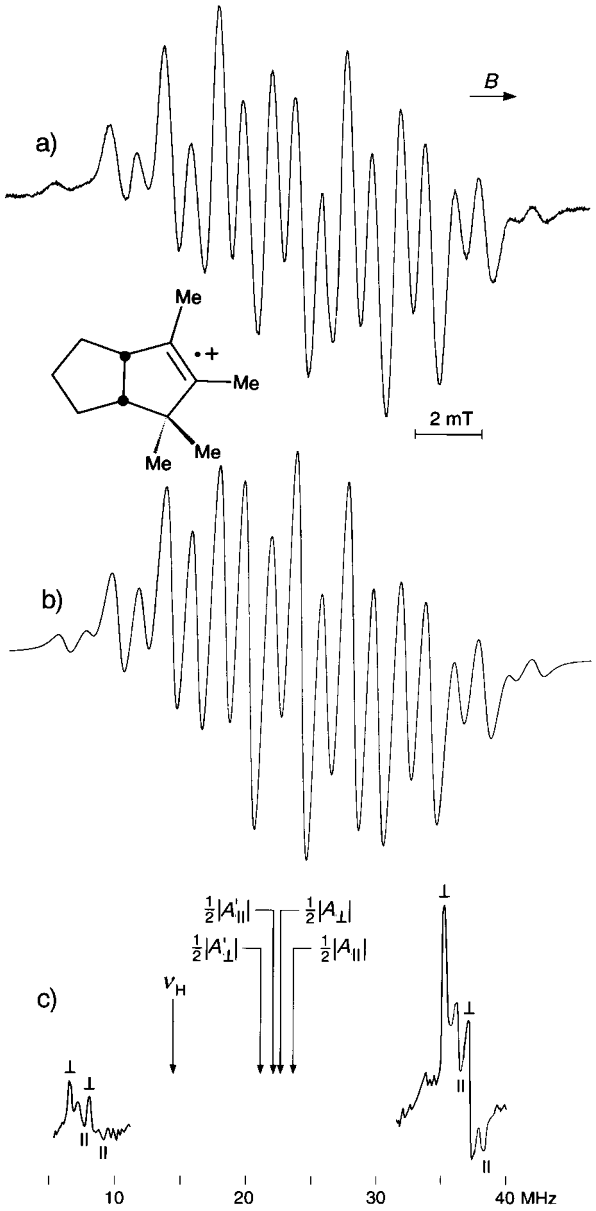

Fig. 1. a) *ESR Spectrum of* **3c**$^{\bullet+}$ *in a CFCl$_3$ matrix at 120 K.* b) *Simulation of the ESR spectrum of* **3c**$^{\bullet+}$ *with the coupling constants given in the text and the* Table (line-shape *Lorentz*ian, line-width 0.7 mT). c) *Parts of ENDOR spectrum of* **3c**$^{\bullet+}$ *in a CFCl$_3$ matrix at 120 K showing the signals from the Me β-protons* (∥ and ⊥).

The same reaction products, **3c**$^{\bullet+}$ (*Fig. 1*) and **2c**$^{\bullet+}$ (*Fig. 2*) of **1c** and **2c**, respectively, were obtained with the three *Freons* CFCl$_3$, CF$_3$CCl$_3$, and CF$_2$ClCFCl$_2$.

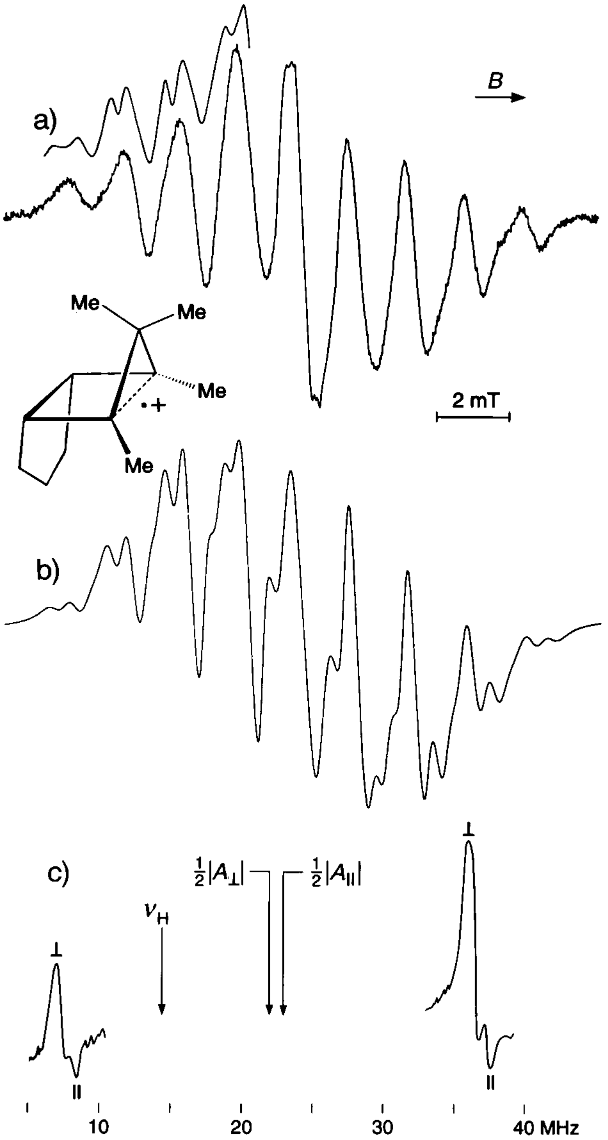

Fig. 2. a) *ESR Spectrum of* **2c**$^{\cdot+}$ *in a* CF_3CCl_3 *matrix at 100 K.* The inserted curve at the low field, showing an additional hyperfine splitting, was recorded at 140 K. b) *Simulation of the ESR spectrum of* **2c**$^{\cdot+}$ *with the coupling constants given in the text and the* Table (line-shape *Lorentz*ian, line-width 0.8 mT). c) *Parts of ENDOR spectrum of* **2c**$^{\cdot+}$ *in a* CF_3CCl_3 *matrix at 100 K showing the signals from the Me β-protons* (ǁ and ⊥).

Cyclobutane Annelation: **1d** *and* **2d**. The ESR and ENDOR spectra observed upon γ-irradiation of the cyclobutane-annelated azoalkane **1d** and housane **2d** in $CFCl_3$ or CF_3CCl_3 matrices resembled those resulting from an analogous treatment of their cyclopentane-annelated counterparts **1c** and **2c**, respectively. The $|a|$ values, verified by computer simulation of the ESR spectra, are 2.68 (1 H), 1.50 (3 H), 1.34 (3 H), and 0.66 mT (1 H) for the reaction product of **1d** and 2.78 (2 H), 1.52 (6 H), and 0.60 mT (2 H) for that of **2d**. These values compare favorably with the corresponding data for **3c**$^{\cdot+}$ and **2c**$^{\cdot+}$ and were, therefore, attributed to the radical cations **3d**$^{\cdot+}$ and **2d**$^{\cdot+}$ of 2,3,4,4-tetramethylbicyclo[3.2.0]hept-2-ene and 2,3,3,4-tetramethylbicyclo[3.2.0]heptane-2,4-diyl, respectively.

A different ESR spectrum was obtained when **1d** and **2d** were γ-irradiated in the 'mobile' $CF_2ClCFCl_2$ matrix. This spectrum, shown in *Fig. 3,a*, could be reproduced by simulation (*Fig. 3,b*) with the use of the $|a|$ values of 2.54 (1 H), 2.13 (3 H), 0.76 (1 H), and 0.73 mT (1 H). It is ascribed to the radical cation **4d**$^{\cdot+}$ of 2,3,3,4-tetramethylcyclohepta-1,4-diene, in which the spin population is localized on one ethene moiety (*Scheme 4*). The corresponding ENDOR spectrum could not be detected.

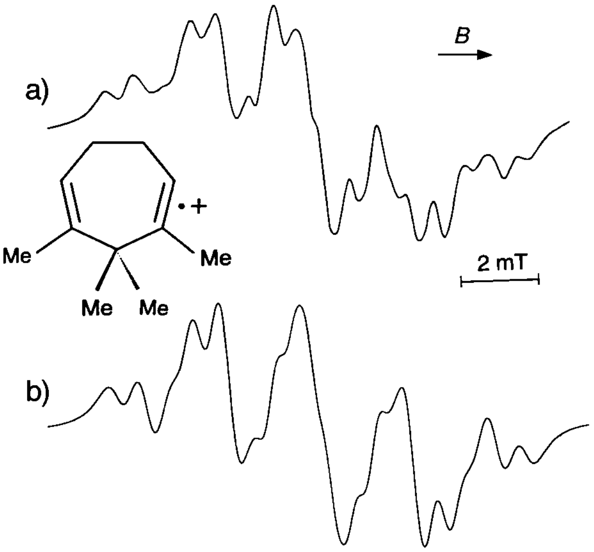

Fig. 3. a) *ESR Spectrum of* **4d**$^{\cdot+}$ *in a* $CF_2ClCFCl_2$ *matrix at 110 K.* b) *Simulation of the ESR spectrum of* **4d**$^{\cdot+}$ *with the coupling constants given in the text and the* Table (line-shape *Lorentz*ian, line-width 0.9 mT).

Cyclobutene Annelation: **1e** *and* **2e**. ESR Spectra of the paramagnetic species produced by γ-irradiation of the cyclobutene-annelated azoalkane **1e** and housane **2e** in *Freon* matrices were rather poorly resolved, but could be analyzed with the aid of the ENDOR technique. They are displayed in *Fig. 4,a*, and *Fig. 5,a*, respectively, above their computer simulations (*Fig. 4,b*, and *Fig. 5,b*) and the corresponding ENDOR spectra (*Fig. 4,c*, and *Fig. 5,c*). In the ionization product of **1e**, β-protons of two distinctly non-equivalent Me substituents give rise to high-frequency components of ENDOR signals at 29.0–30.9 and 35.6–37.5 MHz; the low-frequency partners of the latter are found at 6.6–8.5 MHz (*Fig. 4,c*). In addition, high-frequency components of weaker signals due to α-protons[2]) are observed between 21 and 28 MHz. By contrast, in the ionization product of **2e**, the β-protons of two Me substituents are only slightly

Scheme 4

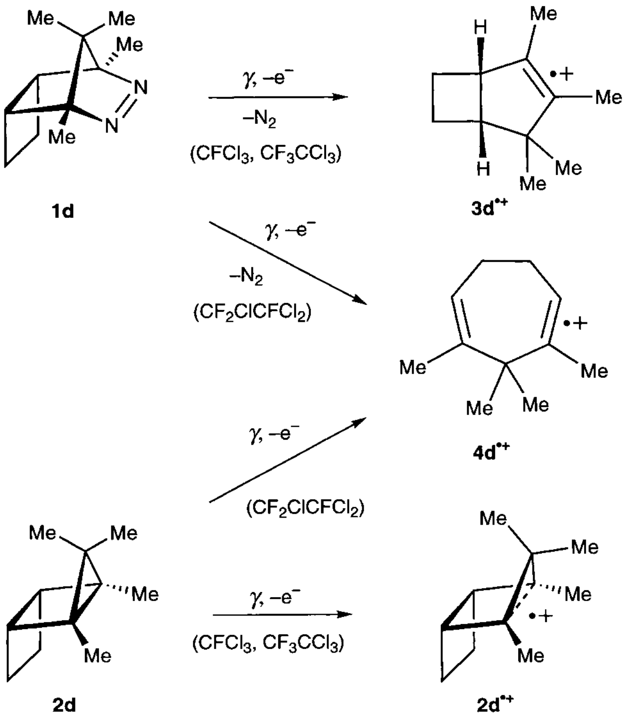

non-equivalent, as the high-frequency components of their signals appear at 26.2–27.6 and 28.3–29.7 MHz. Underlying them, one discerns components of a weaker signal which arises from α-protons (*Fig. 5,c*). The simulations of the ESR spectra were performed with the $|a|$ values of 1.55 (3 H), 1.08 (3 H), 0.85 (1 H), 0.65 (1 H), and 0.50 mT (1 H) for the product of **1e** (*Fig. 4,b*), and of 1.01 (3 H), 0.88 (3 H), and 0.71 mT (2 H) for that of **2e** (*Fig. 5,b*). The pertinent paramagnetic species are considered as the radical cations $\mathbf{4e}^{\cdot+}$ and $\mathbf{4e}'^{\cdot+}$ of the isomeric 1,2,7,7- and 1,6,7,7-tetramethylcyclohepta-1,3,5-trienes, respectively (*Scheme 5*).

When ionization of **1e** and **2e** was carried out in a $CF_2ClCFCl_2$ matrix, ESR spectra of $\mathbf{4e}^{\cdot+}$ and $\mathbf{4e}'^{\cdot+}$ were replaced by hyperfine patterns due to three protons with a substantial $|a|$ value of 2–3 mT. These ESR patterns are presented in *Fig. 4,d*, and *Fig. 5,d*, below the ENDOR spectra of the respective radical cations $\mathbf{4e}^{\cdot+}$ and $\mathbf{4e}'^{\cdot+}$. They are attributed to neutral radicals $\mathbf{5e}^{\cdot}$ and $\mathbf{5e}'^{\cdot}$ formed by addition of $\mathbf{4e}^{\cdot+}$ and $\mathbf{4e}'^{\cdot+}$ to the double bond of **1e** and **2e**, respectively, and loss of a proton (*Scheme 6*).

The pertinent $|a|$ values are 3.06 (2 H) and 2.14 mT (1 H) for $\mathbf{5e}^{\cdot}$, and 2.72 (1 H) and 1.99 mT (2 H) for $\mathbf{5e}'^{\cdot}$. Attempts to observe the corresponding ENDOR spectra failed.

Cyclopropane Annelation: **1f**. γ-Irradiation of the cyclopropane-annelated azoalkane **1f** in *Freon* matrices yielded the ESR spectrum shown in *Fig. 6,a*. Its prominent feature is an extremely large $|a|$ value of 6.60 mT due to two equivalent protons. Such values are known to arise from β-protons of a CH_2 group bridging two sp^2-hybridized

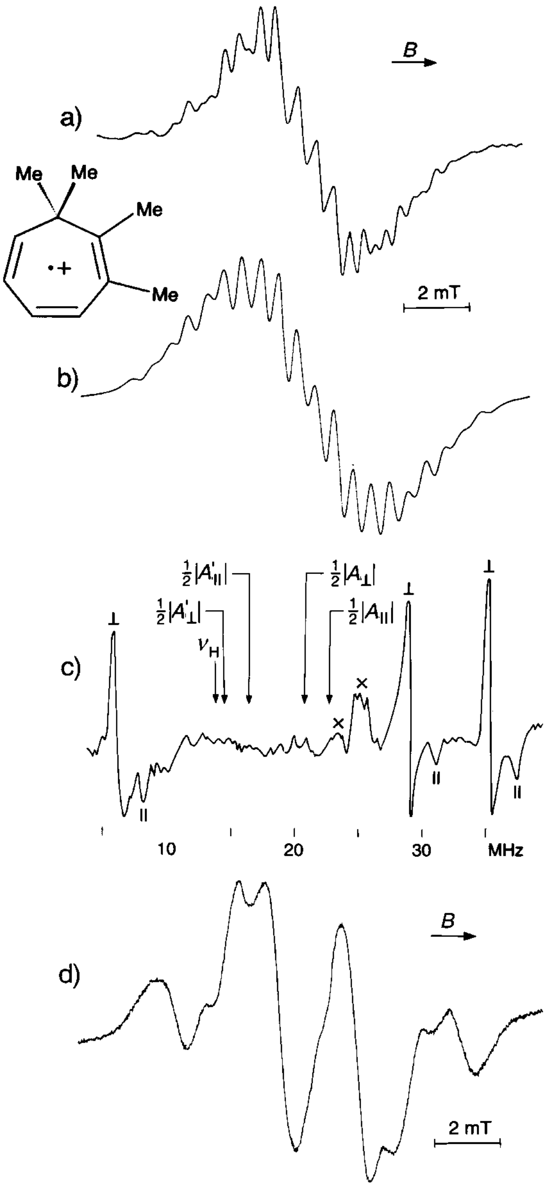

Fig. 4. a) *ESR Spectrum of* **4e**$^{\bullet +}$ *in a* $CFCl_3$ *matrix at 130 K.* b) *Simulation of the ESR spectrum of* **4e**$^{\bullet +}$ *with the coupling constants given in the text and the* Table (line-shape *Lorentz*ian, line-width 0.5 mT). c) *ENDOR Spectrum of* **4e**$^{\bullet +}$ *in a* $CFCl_3$ *matrix at 110 K showing the signals from the Me β-protons* (∥ and ⊥) *and α-protons* (marked by ×). d) *ESR Spectrum of the adduct* **5e**$^{\bullet}$ *in a* $CF_2ClCFCl_2$ *matrix at 118 K.*

C-atoms (π-centers), which bear large LCAO coefficients of the same sign in the singly occupied orbital [8]. An obvious candidate for the paramagnetic species in question is the radical cation **4f**$^{\bullet +}$ of 1,5,6,6-tetramethylcyclohexa-1,4-diene (*Scheme 7*).

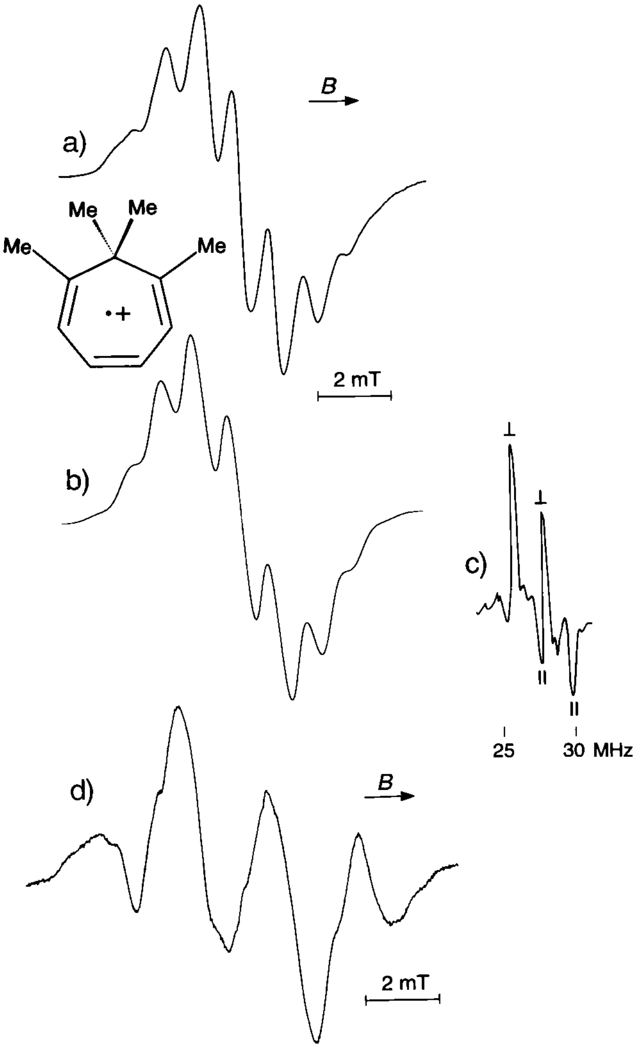

Fig. 5. a) *ESR Spectrum of* **4e′**$^{•+}$ *in a CFCl$_3$ matrix at 110 K.* b) *Simulation of the ESR spectrum of* **4e′**$^{•+}$ *with the coupling constants given in the text and the* Table (line-shape *Lorentz*ian, line-width 0.8 mT). c) *Part of ENDOR Spectrum of* **4e′**$^{•+}$ *in a CFCl$_3$ matrix at 125 K showing the high-frequency signals from the Me β-protons* (|| and ⊥) *and α-protons* (underlying). d) *ESR Spectrum of the adduct* **5e′**$^{•+}$ *in a CF$_2$ClCFCl$_2$ matrix at 118 K.*

The same ESR spectrum (*Fig. 6, a*) was obtained by γ-irradiation of the neutral olefin **4f**, prepared by photolysis of **1f** in *Freon* matrices prior to the radiolytic treatment. The two outer hyperfine components due to the dominating two-proton $|a|$ value of 6.60 mT exhibit a splitting into nine lines that arise from eight protons, of which six are β-protons in the two equivalent Me substituents. The simulation of the ESR spectrum of **4f**$^{•+}$ (*Fig. 6, b*), with the use of the $|a|$ values 6.60 (2 H), 0.67 (6 H), and 0.62 mT (2 H), fails to faithfully reproduce this eight-proton splitting of the central

Scheme 5

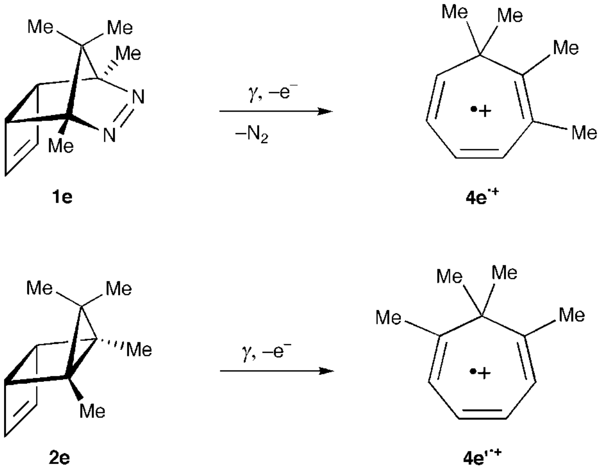

Scheme 6

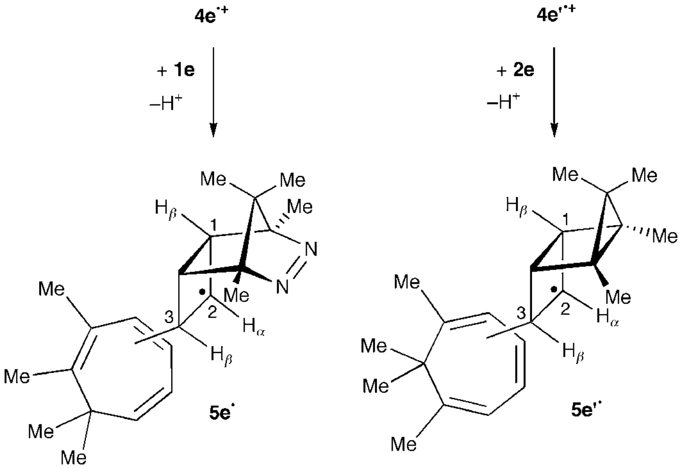

hyperfine component due to 6.60 mT. Obviously, a less extended ESR spectrum of another paramagnetic species was superimposed on that of $\mathbf{4f}^{\bullet+}$; its intensity increased on raising the temperature. The corresponding ENDOR spectrum in *Fig. 6,c*, thus stems from a mixture of $\mathbf{4f}^{\bullet+}$ and this secondary species which is identified as the neutral 1,5,6,6-tetramethylcyclohexadienyl radical ($\mathbf{4f}^{\bullet}$). While the high-frequency components of a signal at 23.4 – 25.6 MHz arise from the six β-protons of the two equivalent Me substituents in $\mathbf{4f}^{\bullet+}$, those at 26.3 – 27.7 MHz must be traced back to such protons in $\mathbf{4f}^{\bullet}$. The high-frequency components of a weaker signal at 29 – 34 MHz are also due to $\mathbf{4f}^{\bullet}$, presumably to an α-proton. A well-resolved ESR spectrum exhibiting a hyperfine pattern, which almost entirely stems from $\mathbf{4f}^{\bullet}$, is reproduced in *Fig. 7,a*. Its computer simulation (*Fig. 7,b*) used the $|a|$ values of 1.29 (1 H), 0.87 (6 H), and 0.23 mT (2 H). This spectrum was obtained upon γ-irradiation of **4f** in a CF_3CCl_3

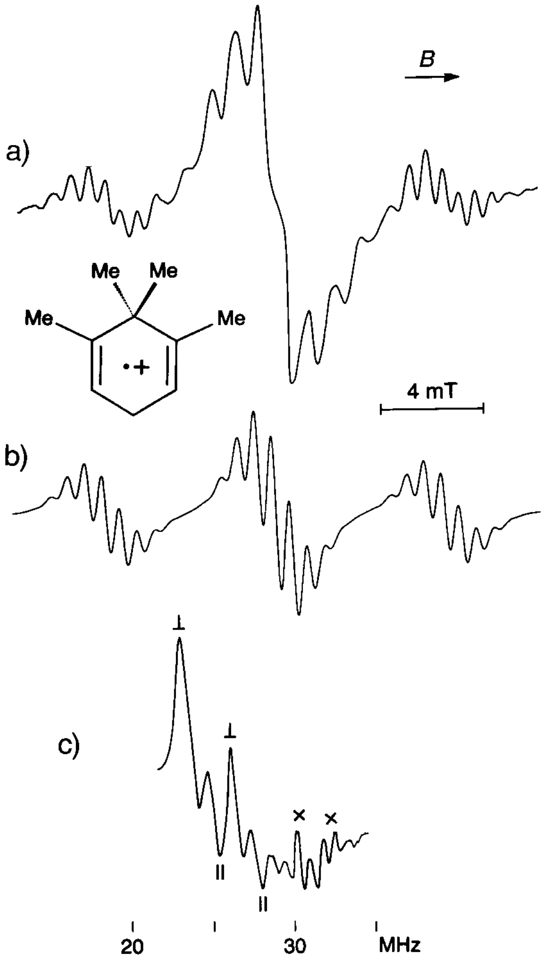

Fig. 6. a) *ESR Spectrum of* **4f**$^{\bullet+}$ (with an admixture of **4f**$^{\bullet}$) *in a* $CFCl_3$ *matrix at 130 K.* b) *Simulation of the ESR spectrum of* **4f**$^{\bullet+}$ *with the coupling constants given in the text and the* Table (line-shape *Lorentz*ian, line-width 0.7 mT). c) *Part of ENDOR spectrum of* **4f**$^{\bullet+}$ (with an admixture of **4f**$^{\bullet}$) *in a* CF_3CCl_3 *matrix at 120 K showing the high-frequency signals from the Me β-protons* (|| and ⊥) *and an α-proton* (marked by ×).

matrix and raising the temperature to 150 K. The pertinent radical **4f**$^{\bullet}$ is presumably a product of several reaction steps. Abstraction of a H-atom from **4f** to give **4f**$^{\bullet}$ might have occurred by the radical $CF_3CCl_2^{\bullet}$ formed by loss of a Cl-atom, as the known 28-line hyperfine pattern of this radical (see, *e.g.*, [9]) appeared intermediately at *ca.* 140 K.

Discussion. – *Assignment of the Coupling Constants.* The *Table* summarizes the ^{1}H-hyperfine data a which were observed for the radical cations and radicals in the present work and to which the proper signs were allotted. (In general, $|a|$ values smaller than 0.3 mT could not be measured.) Specification of the pertinent protons is indicated

Scheme 7

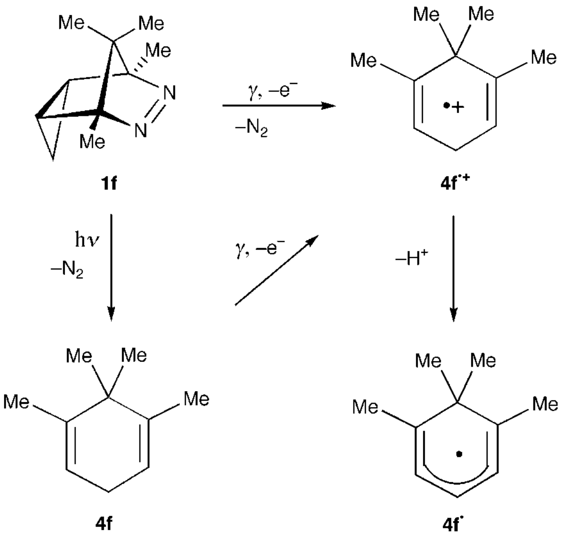

below for all these species with the exception of **5e**$^{\bullet}$, and **5e′**$^{\bullet}$, for which such protons have already been specified in *Scheme 6*. The corresponding coupling constants *a* reported previously for **2a**$^{\bullet+}$ and **2b**$^{\bullet+}$ and **3a**$^{\bullet+}$ and **3b**$^{\bullet+}$ are given for comparison and, to this aim, the numbering of positions in these radical cations was here retained for their annelated derivatives **2c**$^{\bullet+}$ and **2d**$^{\bullet+}$ and **3c**$^{\bullet+}$ and **3d**$^{\bullet+}$.

Calculations by the INDO procedure [10] on the AM1-optimized geometries [11] reproduce well the experimental coupling constants *a*, in particular the larger values for the α- and β-protons. Their assignments are thus guided by the result of these calculations, wherever they cannot unequivocally be made by experiment or by analogy with structurally related species. The signs of *a*, which are required by theory, were confirmed experimentally for those protons that gave rise to anisotropic features ($a > 0$, when $|A_{\|}| > |A_{\perp}|$ and *vice versa* [6][7]).

Apart from **2a**$^{\bullet+}$ and **2b**$^{\bullet+}$, and **3a**$^{\bullet+}$ and **3b**$^{\bullet+}$, hyperfine data for some other paramagnetic species structurally related to the radical cations and radicals dealt with in the present work are found in the literature. They usually refer to unsubstituted species, and can rarely be directly compared with the coupling contants *a* in the *Table*. Among values suitable for such a comparison, one notes the coupling constant +3.8 mT of a β-proton in the radical cation **6**$^{\bullet+}$ of bicyclo[3.2.0]hept-2-ene [12] which resembles +3.89 for **3c**$^{\bullet+}$ and +2.68 mT for **3d**$^{\bullet+}$; an analogous statement holds for the *a* values of the α-protons in the positions 2–5 of the radical cation **7**$^{\bullet+}$ of parent cyclohepta-1,3,5-triene [12][13] with respect to **4e**$^{\bullet+}$ and **4e′**$^{\bullet+}$. In the case of **4e′**$^{\bullet+}$, it is noteworthy that the β-protons of the two Me substituents at C(1) and C(6) have slightly different coupling constants. Such a finding is often encountered with formally equivalent β-protons of radical cations in *Freon* matrices [6][7][14] and points to small deviations from planarity caused by the solid medium. A passable reference for the diene **4d**$^{\bullet+}$ (with the spin population localized on one ethene moiety) is the radical

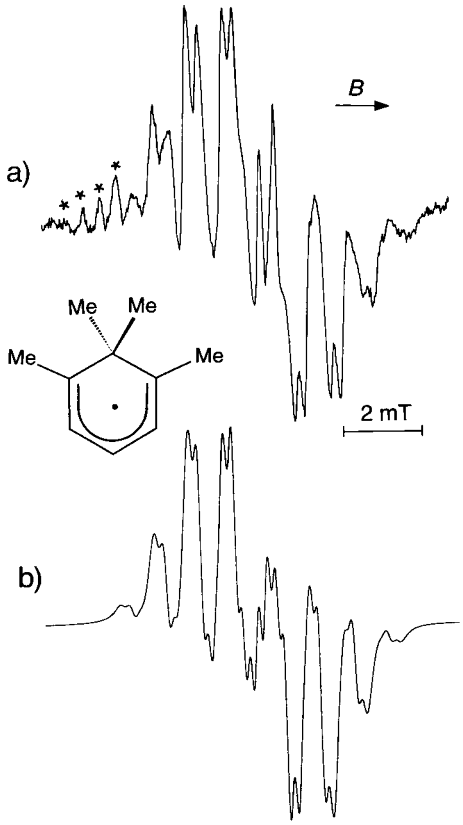

Fig. 7. a) *ESR Spectrum of* **4f**$^{\bullet}$ *in a* CF_3CCl_3 *matrix at 150 K* (the low-field components marked by asterisks stem from $CF_3CCl_2^{\bullet}$). b) *Simulation of the ESR spectrum of* **4f**$^{\bullet}$ *with the coupling constants given in the text and the* Table (line-shape *Lorentz*ian, line-width 0.4 mT).

cation **8**$^{\bullet +}$ of (*Z*)-but-2-ene [15], for which the coupling constants +2.21 mT of the six Me β-protons and −0.98 mT of the two α-protons compare favorably with the analogous values +2.13 and −0.76 mT for **4d**$^{\bullet +}$.

The radical cation **9**$^{\bullet +}$ of cyclohexa-1,4-diene exhibits an extremely large coupling constant, +6.8 [15] (or +6.71 mT [16]), of the four CH_2 β-protons, which is similar to the *a* value, +6.60 mT, of two such protons in **4f**$^{\bullet +}$. Conversion of cyclohexadiene radical cations to cyclohexadienyl radicals is a general phenomenon [6] [15] – [17], and the coupling constants of the α-protons in the position 2–4 of the parent cyclohexadienyl radical (**10**$^{\bullet}$) [6] [16] [18] are almost equal to the corresponding values for **4f**$^{\bullet}$.

Hardly any species closely related to the adducts **5e**$^{\bullet}$ and **5e′**$^{\bullet}$ is, to our knowledge, described in the literature. The simplest reference radical is cyclobutyl (**11**$^{\bullet}$) with the coupling constants, −2.12 and +3.67 mT [18b], of the α- and β-protons, respectively, which are comparable to their counterparts for **5e**$^{\bullet}$ and **5e′**$^{\bullet}$.

Rearrangements. Scheme 8 summarizes the mechanistic outcome obtained in the present work for the diazoalkanes **1c**–**1e** and the housanes **2c**–**2e**. Thus, γ-irradiation

Table 1. *^{1}H-Coupling Constants* a *for Radical Cations and Radicals Derived from the Azoalkanes* **1a**–**1f** *and Housanes* **2a**–**2e**

	T [K]	Matrix		a [mT] a)		
			Position	1,3	4,5-*exo*	2-*anti*
2a$^{\bullet+}$ b)	90	CF_3CCl_3		-1.17 (2 H_α)	$+3.35$ (2 H_β)	$+4.49$ (1 H_β)
2b$^{\bullet+}$ c)	100	$CFCl_3$		$+1.61$ (6 H_β)	$+2.50$ (2 H_β)	$+4.21$ (1 H_β)
2c$^{\bullet+}$	100	CF_3CCl_3		$+1.59$ (6 H_β)	$+2.91$ (2 H_β) d)	
2d$^{\bullet+}$	100	CF_3CCl_3		$+1.52$ (6 H_β)	$+2.78$ (2 H_β) e)	
			Position	1,2	3,5	4-*axial*
3a$^{\bullet+}$ b)	150	$CFCl_3$		-0.94 (2 H_α)	$+4.73$ (4 H_β)	$+0.70$ (2 H_γ)
3b$^{\bullet+}$ c)	105	CF_3CCl_3		-1.06 (1 H_α) $+1.65$ (3 H_β)	$+4.41$ (1 H_β) $+2.44$ (1 H_β) $+2.21$ (1 H_β)	$+0.42$ (2 H_γ)
3c$^{\bullet+}$	120	$CFCl_3$		$+1.65$ (3 H_β) $+1.52$ (3 H_β)	$+3.89$ (1 H_β)	$+0.76$ (1 H_γ)
3d$^{\bullet+}$	110	$CFCl_3$		$+1.50$ (3 H_β) $+1.34$ (3 H_β)	$+2.68$ (1 H_β)	$+0.66$ (1 H_γ)
			Position	1	2	7
4d$^{\bullet+}$ f)	110	$CF_2ClCFCl_2$		-0.76 (1 H_α)	$+2.13$ (3 H_β)	$+2.54$ (1 H_β) $+0.73$ (1 H_β)
			Position	1,6	2,5	3,4
4e$^{\bullet+}$	140	$CFCl_3$		$+1.55$ (3 H_β) -0.85 (1 H_α)	$+1.08$ (3 H_β) < 0.3 g) (1 H_α)	-0.65 (1 H_α) -0.50 (1 H_α)
4e′$^{\bullet+}$	135	$CFCl_3$		$+1.01$ (3 H_β) $+0.88$ (3 H_β)	< 0.3 g) (2 H_α)	-0.71 (2 H_α)
			Position	1,5	2,4	3
4f$^{\bullet+}$	130	$CFCl_3$		$+0.67$ (6 H_β)	-0.62 (2 H_α)	$+6.60$ (2 H_β)
4f$^{\bullet}$	150	CF_3CCl_3		$+0.87$ (6 H_β)	-0.23 (2 H_α)	-1.29 (1 H_α)
			Position	1	2	3
5e$^{\bullet}$	118	$CF_2ClCFCl_2$		$+3.06$ (1 H_β)	-2.14 (1 H_α)	$+3.06$ (1 H_β)
5e′$^{\bullet}$	118	$CF_2ClCFCl_2$		$+2.72$ (1 H_β)	-1.99 (1 H_α)	$+1.99$ (1 H_β)

a) Experimental error in a measured in the present work: ± 0.02 mT. b) Taken from [1b]. c) Taken from [1d]. d) Additional coupling constant a of $+0.55$ mT (2 H_γ) of protons in the annelated cyclopentane ring. e) Additional coupling constant a of $+0.60$ mT (2 H_γ) of protons in the annelated cyclobutane ring. f) Spin population localized on one ethene moiety. g) $|a|$ value too small to be measured (see Text).

of the cyclopentane-annelated housane **2c** yielded throughout the radical cation **2c**$^{\bullet+}$ of 2,3,3,4-tetramethylbicyclo[3.3.0]octane-2,4-diyl. In none of the *Freons* used was rearrangement of **2c**$^{\bullet+}$ *with* a 1,2-Me shift to the corresponding annelated cyclopentene radical cation **3c**$^{\bullet+}$ observed. In contrast, the ionization of the cyclopentane-annelated azoalkane **1c** led, in all the three matrices, to formation of the radical cation **3c**$^{\bullet+}$ of 2,3,4,4-tetramethylbicyclo[3.3.0]oct-2-ene *with* such a shift. Possible precursors such as the diazenyl radical cation **1c**$^{\bullet+}$ or the relatively persistent 1,3-diyl radical cation **2c**$^{\bullet+}$ were not detected, a finding which once again indicates that extrusion of N_2 in diazenyl radical cations **1**$^{\bullet+}$ has to be accompanied by a concerted 1,2-Me shift (*Path A* in *Scheme 8*). Furthermore, the cyclobutane-annelated azoalkane **1d** and housane **2d** gave, in $CFCl_3$ and CF_3CCl_3 matrices, the analogous radical cations **3d**$^{\bullet+}$ and **2d**$^{\bullet+}$ of

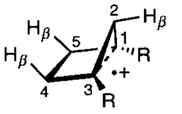

$\mathbf{2a}^{\cdot+}$ $R = H_\alpha$
$\mathbf{2b}^{\cdot+}$ $R = CH_{3,\beta}$

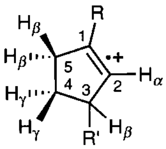

$\mathbf{3a}^{\cdot+}$ $R = H_\alpha$, $R' = H_\beta$
$\mathbf{3b}^{\cdot+}$ $R = CH_{3,\beta}$, $R' = Me$

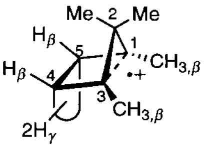

$\mathbf{2c}^{\cdot+}$, $\mathbf{d}^{\cdot+}$

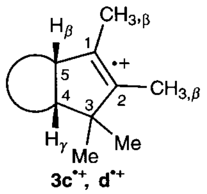

$\mathbf{3c}^{\cdot+}$, $\mathbf{d}^{\cdot+}$

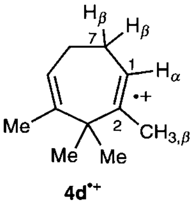

$\mathbf{4d}^{\cdot+}$

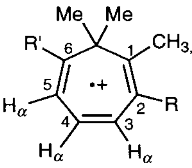

$\mathbf{4e}^{\cdot+}$ $R = CH_{3,\beta}$, $R' = H_\alpha$
$\mathbf{4e'}^{\cdot+}$ $R = H_\alpha$, $R' = CH_{3,\beta}$

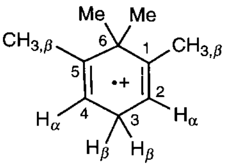

$\mathbf{4f}^{\cdot+}$

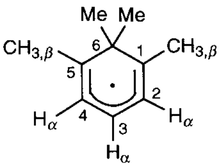

$\mathbf{4f}^{\cdot}$

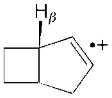

$\mathbf{6}^{\cdot+}$

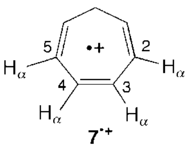

$\mathbf{7}^{\cdot+}$

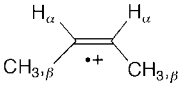

$\mathbf{8}^{\cdot+}$

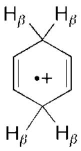

$\mathbf{9}^{\cdot+}$

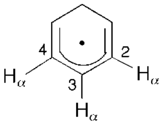

$\mathbf{10}^{\cdot+}$

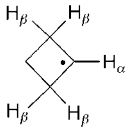

$\mathbf{11}^{\cdot}$

2,3,4,4-tetramethylbicyclo[3.2.0]hept-2-ene and 2,3,3,4-tetramethylbicyclo[3.2.0]heptane-2,4-diyl, respectively. The products $\mathbf{3c}^{\cdot+}$ and $\mathbf{3d}^{\cdot+}$ and $\mathbf{2c}^{\cdot+}$ and $\mathbf{2d}^{\cdot+}$, formed without opening of the annelated ring, are analogous to $\mathbf{3a}^{\cdot+}$ and $\mathbf{3b}^{\cdot+}$ and $\mathbf{2a}^{\cdot+}$ and $\mathbf{2b}^{\cdot+}$, previously obtained from the non-annelated azalkanes **1a** and **1b** and housanes **2a** and **2b** by the same treatment, and the pertinent mechanism has been amply discussed in the literature [1–3]. The diyl radical cations $\mathbf{2c}^{\cdot+}$ and $\mathbf{2d}^{\cdot+}$ are relatively persistent, a property which they share with their non-annelated counterpart $\mathbf{2b}^{\cdot+}$. Evidently, the dimethyl substitution at the diyl-C-atoms, common to all three species, bestow persistence on such radical cations [1d].

Scheme 8

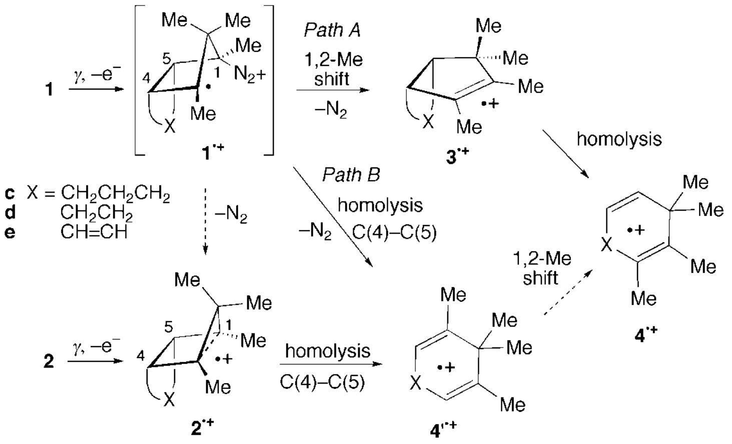

However, opening of the annelated cyclobutane ring (homolysis, *Path B* in *Scheme 8*) to yield the radical cation **4d**$^{\bullet+}$ of 2,3,3,4-tetramethylcyclohepta-1,4-diene occurred on ionization of **1d** and **2d** in the 'mobile' $CF_2ClCFCl_2$ matrix, which is known to facilitate rearrangements. The effect of ring annelation on the products of ionized azoalkanes **1** and the corresponding housanes **2** becomes clearly more pronounced with the decreased size of the annelated ring. This is obvious because, on going from cyclopentane to cyclobutane (and even more so to cyclobutene and cyclopropane; see below), the strain imposed on the C-framework makes an opening of such ring increasingly successful in competition with other reaction paths.

Ring-opened radical cations were the only products obtained from the cyclobutene-annelated azoalkane **1e** and housane **2e**. In this case, the radical cations **4e**$^{\bullet+}$ (from the azoalkane **1e**) and **4e'**$^{\bullet+}$ (from the housane **2e**) of the isomeric 1,2,7,7- and 1,6,7,7-tetramethylcyclohepta-1,3,5-trienes, respectively, were obtained, according to whether a 1,2-Me shift takes place or not. As certified by the experiment on the non-annelated azoalkane **1b** [1d] and its cyclopentane- and cyclobutane-annelated counterparts **1c** and **1d**, such a shift is favored when starting from the azoalkane **1e** but not from the housane **2e**. Yet, in none of our experiments were hints of the existence of the pertinent radical cation **3e**$^{\bullet+}$ of 2,3,4,4-tetramethylbicyclo[3.2.0]hepta-2,6-diene found. This can be rationalized in terms of **3e**$^{\bullet+}$ being non-persistent under the conditions of our experiments which favor further conversion to the radical cation **4e**$^{\bullet+}$ of 1,2,7,7-tetramethylcyclohepta-1,3,5-triene. It is noteworthy that the radical cation of unsubstituted bicyclo[3.2.0]hepta-2,6-diene, the parent of its elusive tetramethyl derivative **3e**$^{\bullet+}$, was identified by its ESR spectrum either on direct ionization of the neutral compound [12], or on rearrangement of the ionized quadricyclane and norbornadiene [13]. However, and most significantly, this unsubstituted radical cation undergoes ring opening to cyclohepta-1,3,5-triene (**7**$^{\bullet+}$) at 113 K in a $CFCl_3$ matrix [12]. Applied to the case of **3e**$^{\bullet+}$, such a finding means that the tetramethyl-substitution of bicyclo[3.2.0]-hepta-2,6-diene destabilizes the pertinent radical cation, at least under conditions of matrix isolation. In contrast to the corresponding azoalkane **1e**, opening (homolysis) of the annelated cyclobutene ring *without* 1,2-Me migration represents the exclusive reaction path for the 1,3-diyl radical cation **2e**$^{\bullet+}$ and affords the isomeric 1,6,7,7-substituted radical cation **4e′**$^{\bullet+}$. Only in the 'mobile' $CF_2ClCFCl_2$ matrix, the primarily observed radical cations **4e**$^{\bullet+}$ and **4e′**$^{\bullet+}$ were replaced by the adducts **5e**$^{\bullet}$ and **5e′**$^{\bullet}$, formed by addition of **4e**$^{\bullet+}$ and **4e′**$^{\bullet+}$ to the double bond of **1e** and **2e**, respectively, and the subsequent loss of a proton. Such a bimolecular reaction might be expected to occur in frozen $CF_2ClCFCl_2$, and it is attributed to the typical property of this 'mobile' matrix.

A behavior upon ionization that differs from that of the azoalkanes **1c** – **1e** was observed for the cyclopropane-annelated **1f**, the most strained compound in the series. Particularly revealing is the comparison of such a behavior of **1f** to that of its cyclobutene-annelated counterpart **1e**. Whereas the reaction path for the ionized azoalkane **1e** was recognized as a 1,2-Me shift followed by opening (homolysis) of the cyclobutene ring to **4e**$^{\bullet+}$, the analogous path for **1f**, *via* the transient **1f**$^{\bullet+}$, is the opening of the cyclopropane ring to the radical cation **4f**$^{\bullet+}$ of 1,5,6,6-tetramethylcyclohexa-1,4-diene, apparently *without* a 1,2-Me shift. Clearly, the maximal strain imposed on the C-framework by the annelated three-membered ring in **1f** overwhelmingly favors the opening of this ring on ionization in competition with all other reaction paths accessible to **1c** – **1e**, even such as the 1,2-Me shift. The special status of **1f** as the azoalkane with the smallest annelated ring is further documented by its photolysis which yields directly the 1,5,6,6-tetramethylcyclohexa-1,4-diene (**4f**) without formation of the housane precursor **2f**.

This work was supported by the *Swiss National Science Foundation.*

REFERENCES

[1] a) K. Ushida, T. Shida, J. C. Walton, *J. Am. Chem. Soc.* **1986**, *108*, 2805; b) F. Williams, Q.-X. Guo, T. M. Kolb, S. F. Nelsen, *J. Chem. Soc., Chem. Commun.* **1989**, 1835; c) W. Adam, H. Walter, G.-F. Chen, F. Williams, *J. Am. Chem. Soc.* **1992**, *114*, 3007; d) W. Adam, C. Sahin, J. Sendelbach, H. Walter, G.-F. Chen, F. Williams, *J. Am. Chem. Soc.* **1994**, *116*, 2576.

[2] a) W. Adam, T. Oppenländer, G. Zang, *J. Org. Chem.* **1985**, *50*, 3303; b) S. C. Blackstock, J. K. Kochi, *J. Am. Chem. Soc.* **1987**, *109*, 2484; c) W. Adam, U. Denninger, R. Finzel, F. Kita, H. Platsch, H. Walter, G. Zang, *J. Am. Chem. Soc.* **1992**, *114*, 5027; d) W. Adam, C. Sahin, *Tetrahedron Lett.* **1994**, *35*, 9027; e) W. Adam, T. Heidenfelder, C. Sahin, *J. Am. Chem. Soc.* **1995**, *117*, 9693; f) W. Adam, A. Corma, M. A. Miranda, M.-J. Sabater-Picot, C. Sahin, *J. Am. Chem. Soc.* **1996**, *118*, 2380.

[3] a) D. E. Reedich, R. S. Sheridan, *J. Am. Chem. Soc.* **1988**, *110*, 3697; b) J. S. Adams, R. B. Weisman, P. S. Engel, *J. Am. Chem. Soc.* **1990**, *112*, 9115; c) C. J. S. M. Simpson, G. J. Wilson, W. Adam, *J. Am. Chem. Soc.* **1991**, *113*, 4728.

[4] L. A. Paquette, L. M. Leichter, *J. Am. Chem. Soc.* **1971**, *93*, 4922, 5128; b) L. A. Paquette, L. M. Leichter, *J. Org. Chem.* **1974**, *39*, 461.

[5] a) K. Beck, A. Höhn, S. Hünig, F. Prokschy, *Chem. Ber.* **1984**, *117*, 517; b) K. Beck, S. Hünig, *Chem. Ber.* **1987**, *112*, 477; c) W. Adam, T. Heidenfelder, C. Sahin, *Synthesis* **1995**, 1163.

[6] A. Arnold, U. Burger, F. Gerson, E. Kloster-Jensen, S. P. Schmidlin, *J. Am. Chem. Soc.* **1993**, *115*, 4271.

[7] F. Gerson, *Acc. Chem. Res.* **1994**, *27*, 63.

[8] D. H. Whiffen, *Mol. Phys.* **1993**, *6*, 223; see also: F. Gerson, X.-Z. Qin, C. Ess, E. Kloster-Jensen, *J. Am. Chem. Soc.* **1989**, *111*, 6456.

[9] F. Gerson, P. Merstetter, M. Mascal, N. M. Hext, *Helv. Chim. Acta* **1998**, *81*, 1749.

[10] J. A. Pople, D. L. Beveridge, 'Approximate Molecular Orbital Theory', McGraw-Hill, New York, 1970.

[11] M. J. S. Dewar, E. G. Zoebisch, E. F. Healy, J. J. P. Stuart, *J. Am. Chem. Soc.* **1985**, *107*, 3902.

[12] A. Faucitano, A. Buttatava, F. Marinotti, R. Sustmann, H.-G. Korth, *J. Chem. Soc.*, *Perkin Trans. 2* **1992**, 865.
[13] G.-F. Chen, J.-T. Wang, F. Williams, K. D. Belfield, J. E. Baldwin, *J. Am. Chem. Soc.* **1991**, *113*, 9853.
[14] J.-N. Aebischer, T. Bally, K. Roth, E. Haselbach, F. Gerson, X.-Z. Qin, *J. Am. Chem. Soc.* **1989**, *111*, 7909.
[15] T. Shida, Y. Egawa, H. Kubodera, T. Kato, *J. Chem. Phys.* **1980**, *73*, 5963.
[16] M. Tabata, A. Lund, *Chem. Phys.* **1983**, *75*, 379.
[17] M. Shiotani, *Magn. Reson. Rev.* **1987**, *12*, 333.
[18] R. W. Fessenden, R. H. Schuler, *J. Chem. Phys.* **1963**, *38*, 773; b) R. W. Fessenden, R. H. Schuler, *J. Chem. Phys.* **1963**, *39*, 2147.

Received April 2, 2001